# Simulating complex flows of liquid-crystalline polymers using the Doi theory

J. Feng[a] and L. G. Leal

*Department of Chemical Engineering, University of California–Santa Barbara, Santa Barbara, California 93106-5080*

(Received 2 May 1997; final revision received 6 August 1997)

**Synopsis**

We simulate the startup flow of lyotropic liquid-crystalline polymers (LCPs) in an eccentric cylinder geometry. The objectives are to explore the mechanisms for the generation of disclinations in a nonhomogeneous flow and to study the coupling between the flow and the polymer configuration. The Doi theory, generalized to spatially varying flows and approximated by the quadratic closure, is used to model the evolution of LCP configurations. This, along with the equations of motion for the fluid, is solved by a finite-element method. The flow modification by the polymer stress is mild for the parameters used, but the LCP exhibits complex orientational behavior in different regions of the flow domain. For relatively weak nematic strength, a steady state is reached in which the director is oriented either along or transverse to the streamline, depending upon local flow conditions and the deformation history. A pair of disclinations, with strength $\pm 1/2$, are identified in the steady state, and the LCP configuration at the disclinations confirms the model of a structured defect core proposed by Greco and Marrucci (1992). For strong nematic strength, director tumbling occurs in the more rotational regions of the flow field, giving rise to a polydomain structure. The boundary of the tumbling domain consists of two disclinations of $\pm 1/2$ strength, a structure very similar to previous experimental observations of LCP domains.  [S0148-6055(97)00306-4]

## I. INTRODUCTION

In 1971, DuPont produced ultrahigh strength Kevlar® fibers from liquid-crystalline polyamides. Since then, the prospect of using liquid-crystalline polymers (LCPs) as structural and barrier materials has spawned intensive research efforts. To date, however, the high expectations of LCPs remain largely unfulfilled. Commercial production of LCPs other than fibers has been limited to injection molding of very small high-precision parts. These operations take advantage of the low processing viscosity and small thermal expansion of LCPs, but not the high tensile strength and moduli that come with optimal orientation of LCP molecules. The main difficulty in molding three-dimensional parts consists in controlling molecular orientation. A major problem is the tendency for formation and proliferation of disclinations under flow, leading to so-called polydomain structures. The goal of controlling molecular orientation requires a thorough understanding of the rheology and flow behavior of these peculiar materials as well as advanced strategies for mold design and process optimization [Ophir and Ide (1983)].

[a]Corresponding author.

Lyotropic LCPs (solutions) are easier to study than thermotropics (melts) and, thus, our knowledge is more complete for lyotropics. The rheology of the two types of LCPs differs in certain aspects, and in this paper, we will focus on lyotropics. Most of the prior research on LCP rheology has been done on simple shear flows. Based on rheological measurements and optical observations, a more or less complete picture of LCP behavior in shear flow has emerged [Larson and Mead (1993)], which consists of an Ericksen number cascade and a Deborah number cascade. The first cascade comprises flow regimes at low-to-medium shear rates for which the LCP behavior is governed by the balance between a viscous torque due to flow and an elastic torque due to Frank elasticity. The relative magnitude of these two torques is represented by the Ericksen number $Er$. As $Er$ increases, the LCP behavior evolves from steady tipping of the director in the shear plane to a roll-cell instability and director turbulence. The Leslie–Ericksen (LE) theory [Leslie (1979)], along with elastic and flow stability analyses based on the LE theory [Pieranski *et al.* (1976); Larson (1993)], describes the low $Er$ regimes well, although the physics behind the generation of disclination lines is still unknown. In the polydomain regime of director turbulence, domain refinement and transient rheology may be described by the mesoscopic Larson–Doi theory [Larson and Doi (1991)]. The regime of director turbulence corresponds to region II of the often cited Onogi–Asada flow curve [Onogi and Asada (1980)]. The low $Er$ behavior described above is for well-relaxed or monodomain initial states, and does not correspond to the shear-thinning region I. The origin for region I remains a mystery; recent experiments have suggested a few possibilities [Walker and Wagner (1994); Ugaz *et al.* (1997)].

At higher flow rates, the molecular order is distorted by the flow, giving rise to a molecular elasticity that overwhelms the Frank elasticity. At this stage, the LCP configuration is governed by the competition between flow-induced distortion and relaxation through Brownian motion, indicated by the Deborah number $De$. The monodomain Doi theory predicts tumbling, wagging, and flow-aligning behavior of LCPs at increasing shear rate [Marrucci (1990); Larson (1990)]. Even though the polydomain structure persists except for the highest flow rates, the elastic stress between domains is apparently unimportant; an average over individual tumbling/wagging domains predicts steady-state rheological properties such as shear viscosity and normal stress differences [Marrucci and Maffettone (1990); Larson (1990)]. These predictions are in good qualitative and sometimes quantitative agreement with experiments [Magda *et al.* (1991); Baek *et al.* (1993a, 1993b)]. The $De$ cascade corresponds to region III of the Onogi–Asada flow curve.

Homogeneous flows other than simple shear have received much less attention. Purely extensional flow of LCPs is simple because of the uniform alignment of molecules with the streamlines [See *et al.* (1990)]. Homogeneous flows of a mixed type have been considered by Chaubal *et al.* (1995). The most interesting result is that the behavior of LCPs is extremely sensitive to the flow type in the neighborhood of simple shear. The slightest addition of an extensional component to a simple shear flow will change director tumbling to flow aligning. Conversely, adding a small rotational component will lead to tumbling up to very large Deborah numbers.

Nonhomogeneous flows are more complex than homogeneous flows for two reasons: the presence of history effects due to the Lagrangian unsteadiness of the flow and flow modification due to nonzero divergence of the polymer contribution to stress. The polymer configuration, represented by the orientation distribution function, depends on the deformation history in any flow. But for nonhomogeneous flows, this dependence is particularly significant since the flow conditions vary both along and between streamlines. The coupling between flow and polymer configuration is a hallmark of nonhomogeneous flows. Grizzuti *et al.* (1991) observed modification of the velocity field in a slit

flow of LCP solutions. There is a local maximum of the velocity near the edges of the channel, indicating lower viscosity there. This is consistent with later studies by Bedford and Burghardt (1994, 1996) who demonstrated that the LCP molecules are almost perfectly aligned with the flow near the sidewalls. These latter authors did not, however, detect any significant flow modification. More complex geometries, such as channels with abrupt or gradual expansion/contraction, have been studied by Baleo and Navard (1994) and Bedford and Burghardt (1996). Besides the strong alignment near the sidewalls, both studies confirmed that converging flows tend to align LCP molecules and enhance orientational order.

In summary, the behavior of LCPs in shear flows has been well documented in experiments but theoretical development lags experiments. The Doi theory applies at high flow rates when the elastic stress due to gradients of the director field is unimportant. The monodomain assumption, however, precludes the theory from accounting for the generation and proliferation of disclinations at lower flow rates. For nonhomogeneous LCP flows, recent experiments have provided some insights, but at present, there is no detailed and accurate understanding of the coupling between flow and LCP configurations. There is a wide gap between our modeling capability of LCP flows and the goal of injection molding high-strength three-dimensional parts.

A critical task then appears to be to develop a new theory to accommodate the dynamics of disclinations and the polydomain structure. Marrucci and Greco (1991, 1992, 1993) made a breakthrough in this direction. By using a nematic potential with nonlocal molecular interactions, they added the elasticity due to spatial variation of the polymer configuration to the Doi theory. This effect reduces to the Frank elasticity in the limit of weak flows. The new potential introduces spatial interaction in the director field, and hence, the possibility of theoretically accounting for wall anchoring. The new theory admits a ''hedgehog defect'' as a solution in the absence of flow [Greco and Marrucci (1992)], but so far has not been used for flow calculations.

The work to be presented in this paper takes a different approach. We relax the monodomain restriction of the Doi theory, as suggested by Marrucci and Greco (1993), by allowing the polymer configuration and the flow to vary in space. Then, instead of adding gradient elasticity, we test the theory in nonhomogeneous flow simulations. In an eccentric cylinder device, the theory predicts disclination lines of half-strength and a tumbling domain whose boundary is made up of such disclination lines. Similar extensions of the Doi theory were previously attempted in channel flows [Armstrong *et al.* (1995); Mori *et al.* (1995)] and Couette flows [Wang (1996)]. Because of the flow kinematics or limitations to high Peclet numbers, only monodomain, steady solutions have been obtained.

In the next section, we will define the flow problem and formulate the governing equations. The Stokes flow kinematics are described in Sec. III. LCP flows with steady and periodic director motions are discussed in Secs. IV and V. Conclusions will be given in the final section.

## II. FORMULATION OF THE PROBLEM

We consider the start-up flow in an eccentric cylinder device (Fig. 1). This geometry is used because it contains extensional, shear and rotational flows in different regions; this affords us the opportunity to examine how the LCP configuration evolves along streamlines that pass through different regions. The outer cylinder is stationary and the inner cylinder starts at time $t = 0$ to rotate with angular velocity $\omega$. The geometry is characterized by two dimensionless parameters: $\mu = (R_2 - R_1)/R_1 = 7/3$ and $\epsilon$

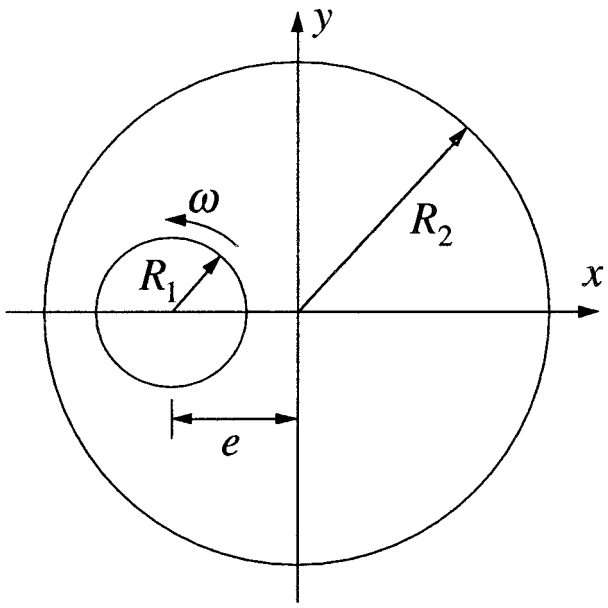


**FIG. 1.** The eccentric cylinder device.

$= e/R_1 = 5/3$. In presenting the results, we will take $R_1 = 3$ and $R_2 = 10$ so as to avoid fractional radii. This amounts to using $\Lambda = R_1/3$ as the characteristic length.

Doi (1981) modeled an LCP solution as a concentrated suspension of rodlike molecules with uniform length $L$ and negligible thickness. The orientation distribution of the polymer and the velocity gradient were assumed to be spatially uniform. A generalization to spatially nonuniform systems was formulated by Doi and Edwards (1986), allowing translation of polymer molecules by diffusion and convection. In this paper, we neglect translational diffusion so as to maintain a uniform polymer concentration in the solution. If we then apply the Prager procedure to the Smoluchowski equation [Eq. (8.26) of Doi and Edwards (1986)], the evolution equation of the second moment tensor is obtained:

$$\frac{\partial \mathbf{A}}{\partial t} + \mathbf{v}\cdot\nabla\mathbf{A} - \nabla\mathbf{v}^T\cdot\mathbf{A} - \mathbf{A}\cdot\nabla\mathbf{v} = -6D_r\left(\mathbf{A} - \frac{\delta}{3}\right) + 6UD_r(\mathbf{A}\cdot\mathbf{A} - \mathbf{A}:\mathbf{AA}) - 2\mathbf{D}:\mathbf{AA}, \tag{1}$$

where $\mathbf{A} = \langle \mathbf{uu} \rangle$, $\mathbf{u}$ being the unit vector along the axis of the molecules. $\delta$ is the unit tensor, $\mathbf{v}$ is the fluid velocity, and $\mathbf{D}$ is the deformation gradient tensor $\mathbf{D} = (\nabla\mathbf{v} + \nabla\mathbf{v}^T)/2$. $D_r$ is the rotational diffusivity of the LCP molecules, and the dimensionless parameter $U$ is the nematic strength in the Maier–Saupe potential

$$V(\mathbf{u}) = -\tfrac{3}{2}UkT\mathbf{uu}:\mathbf{A}, \tag{2}$$

where $k$ is the Boltzmann constant and $T$ the temperature.

A few comments about Eq. (1) are in order. First, the $(\mathbf{v}\cdot\nabla\mathbf{A})$ term describes the spatial variation of $\mathbf{A}$ along a streamline, and is not included in the monodomain Doi theory. A similar derivation of this term was given by Bhave *et al.* (1991). Second, we have neglected the tube dilation effect, namely, the enhanced diffusivity due to molecular order. We have carried out simulations with tube dilation and the results do not differ qualitatively for the parameters used. Third, the quadratic closure is used, mostly for its

simplicity. Its often-mentioned failure to predict director tumbling in simple shear is not a serious problem for other types of homogeneous flows [Chaubal *et al.* (1995)]. In a nonhomogeneous flow, the history effect will further reduce the influence of the local flow properties, and the choice of closure approximations is expected to be less consequential. Finally, Eq. (1) is formulated in terms of $\mathbf{A} = \langle \mathbf{uu} \rangle$ instead of the order parameter tensor $\mathbf{S} = \mathbf{A} - \delta/3$. $\mathbf{A}$ is positive definite and, thus, can be geometrically represented by an ellipsoid; this facilitates graphical presentation of the results. We will refer to $\mathbf{A}$ as the configuration tensor since it contains all the information about the orientation distribution function at this level of approximation.

For the polymer stress, we adopt the original form of Doi (1981):

$$\tau = 3\nu kT\left(\mathbf{A} - \frac{\delta}{3}\right) - 3\nu kTU(\mathbf{A}\cdot\mathbf{A} - \mathbf{A}:\mathbf{AA}) + \frac{\nu kT}{2D_r(\nu L^3)^2}\mathbf{D}:\mathbf{AA}, \tag{3}$$

where $\nu$ is the number density of the rodlike molecules. Equation (3) does not take into account the inhomogeneity of $\mathbf{A}$. In other words, we have neglected any dependence of $\tau$ on $\nabla\mathbf{A}$. The term proportional to $\mathbf{D}:\mathbf{AA}$ is a viscous stress, $(\nu L^3)^2$ being the crowdedness factor. [One referee pointed out that an empirical coefficient $\beta = O(10^3)$ should multiply the viscous stress (see Sec. 9.4.3 of Doi and Edwards, 1986). Fortunately, this does not invalidate our results since the crowdedness factor $(\nu L^3)^2$ is determined empirically by comparing the viscous stress as in Eq. (3) to experimental data, and thus, will incorporate the $\beta$ factor.]

Assuming negligible inertia, we write the governing equations for the fluid flow as

$$\nabla\cdot\mathbf{v} = 0, \tag{4}$$

$$\rho\frac{\partial\mathbf{v}}{\partial t} = -\nabla p + \eta_s\nabla^2\mathbf{v} + \nabla\cdot\tau, \tag{5}$$

where $\rho$ is the density of the fluid, $\eta_s$ is the solvent viscosity, and $p$ is the pressure.

Equations (1) and (3) can be made dimensionless:

$$\frac{\partial\mathbf{A}}{\partial t} + \mathbf{v}\cdot\nabla\mathbf{A} - \nabla\mathbf{v}^T\cdot\mathbf{A} - \mathbf{A}\cdot\nabla\mathbf{v} = -\frac{1}{Pe}\left(\mathbf{A} - \frac{\delta}{3}\right) + \frac{U}{Pe}(\mathbf{A}\cdot\mathbf{A} - \mathbf{A}:\mathbf{AA}) - 2\mathbf{D}:\mathbf{AA}, \tag{6}$$

$$\tau = \left(\mathbf{A} - \frac{\delta}{3}\right) - U(\mathbf{A}\cdot\mathbf{A} - \mathbf{A}:\mathbf{AA}) + \frac{Pe}{(\nu L^3)^2}\,\mathbf{D}:\mathbf{AA}, \tag{7}$$

where the strain rate is scaled by $\omega$, the length by $\Lambda = R_1/3$, the velocity $\mathbf{v}$ by $\omega\Lambda$, time $t$ by $\omega^{-1}$, and the polymer stress by $3\nu kT$. The Peclet number is defined by $Pe = \omega/(6D_r)$; it is also the Deborah number since $1/D_r$ may be considered the relaxation time of the polymer molecules. The equation of motion for the fluid flow is made dimensionless by scaling $p$ by $\eta_s\omega$:

$$Re\frac{\partial\mathbf{v}}{\partial t} = -\nabla p + \nabla^2\mathbf{v} + \frac{c}{Pe}\,\nabla\cdot\tau, \tag{8}$$

where the Reynolds number is defined as $Re = \rho\omega\Lambda^2/\eta_s$, and

$$c = \frac{\nu kT}{2\eta_s D_r}, \tag{9}$$

is a concentration parameter. The physical meaning of $c$ needs some explanation. It is proportional to the polymer contribution to the zero-shear-rate viscosity of the LCP solution. The Doi theory gives this contribution as

$$\eta_p = \frac{\nu kT}{6D_r}\frac{(1-S)^2(1+2S)(1+\frac{3}{2}S)+[3/2(\nu L^3)^2]S^2(1+2S)(1-S)}{(1+S/2)^2} = \frac{\nu kT}{2D_r}\alpha(S), \tag{10}$$

where $S = [(3\mathbf{A}:\mathbf{A}-1)/2]^{1/2}$ is the order parameter. Thus, $\eta_p/\eta_s = \alpha(S)c$. If the LCP molecules are well aligned (by strong nematic strength $U$, say), $\alpha$ can be very small. The polymer contribution to the shear viscosity is then much smaller than $c$.

So our problem is completely defined by Eqs. (6)–(8). The dimensionless parameters are: $Re$, $Pe$, $U$, $c$, and $(\nu L^3)^2$ along with two geometric parameters of the eccentric cylinder device $\mu$ and $\epsilon$. The Reynolds number is proportional to the time scale for the suspending fluid to react, via vorticity diffusion, to a change of speed at the inner cylinder. To avoid the complication of this flow transient, we fix the Reynolds number at a small value $Re = 1.11\times10^{-4}$. To select appropriate values for $c$ and $(\nu L^3)^2$, we refer to the measurements on aqueous hydroxypropylcellulose solutions reported by Doraiswamy and Metzner (1986) and Mori *et al.* (1995). The crowdedness parameter ranges from $O(10^2)$ to $O(10^3)$, and $c = O(10^6)$ owing to the small solvent viscosity in their systems. In our computations, we fix $(\nu L^3)^2 = 200$, but use $c = 10$ and 100. The small $c$ values are intended to suppress flow modification effects. As will become clear in the next section, the dynamics of the polymer configuration is rather complicated. By avoiding the complication of severe flow modifications in this initial study, the LCP behavior is easier to analyze. For larger $c$ values, the coupling between LCP configuration and the fluid flow will be stronger. But the dynamics of LCP orientation and ordering that the current study reveals will apply. The remaining parameters, $Pe$ and $U$, will be varied so as to generate steady and periodic regimes of director motion.

The flow field is two-dimensional in the $x-y$ plane. The individual molecules are allowed to orient out of the plane but maintain a collective symmetry about the plane. So the director is either in the plane or perpendicular to it, the latter corresponding to a log-rolling state. The imposed symmetry excludes the kayaking regime that is observed in simple shear over a narrow range of parameters [Larson and Öttinger (1991)].

The no-slip boundary condition is used on solid walls. No boundary condition is needed for **A** because of the hyperbolic nature of Eq. (6); **A** evolves along the characteristics, which are the streamlines. This is an inherent shortcoming of the Doi theory since director anchoring cannot be accommodated. Subject to the symmetry about the flow plane, the configuration tensor **A** has three unknown components:

$$\mathbf{A} = \begin{bmatrix} A_1 & A_2 & 0 \\ A_2 & A_3 & 0 \\ 0 & 0 & 1-A_1-A_3 \end{bmatrix}. \tag{11}$$

The initial order parameter is taken to be the equilibrium value [Doi (1981)]:

$$S_{\text{eq}} = \frac{1}{4}+\frac{3}{4}\left(1-\frac{8}{3U}\right)^{1/2}. \tag{12}$$

Initially, the director is uniformly aligned with one of the $x$, $y$, and $z$ axes.

The numerical algorithm is adapted from a code that we have used to compute two-dimensional flow of dilute polymer solutions [Feng and Leal (1997)]. The flow solver

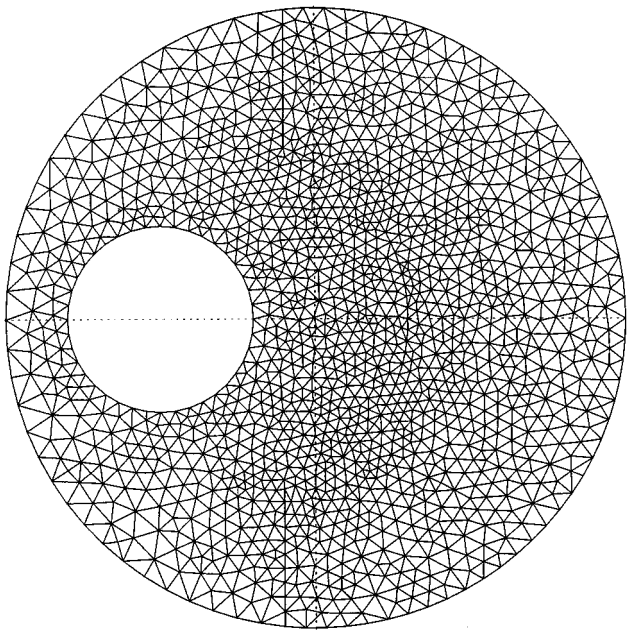

**FIG. 2.** A typical mesh used in the simulations, with 2872 triangular elements, 5868 nodes, and 1498 vertices.

needs little change, but the evolution equation for **A** is more complicated for LCPs than FENE dumbbells. The coupled system [Eqs. (6)–(8)] is solved by using a finite-element method on an unstructured triangular mesh, an example of which is shown in Fig. 2. A special feature of the program is the treatment of the convection term ($\mathbf{v}\cdot\nabla\mathbf{A}$); it is discretized implicitly or explicitly on different nodes depending on the property of the tensor **A**. This ensures that the eigenvalues of **A** lie in the range of (0,1). For a few sets of parameters, we did numerical experiments to ensure convergence of the solution with respect to the mesh size and the time step. Our numerical algorithm allows us access to a much wider range of parameters than was accessible to Mori *et al.* (1995). In particular, we can compute sufficiently low Peclet numbers that director tumbling occurs in the more rotational regions of the flow.

## III. STOKES FLOW

A Stokes flow prevails in the absence of polymer stresses. This flow field serves as a base line in identifying flow modification by polymer stresses. Besides, since flow modification is mild for the parameters used in this study, most features of the Stokes flow carry over to the LCP flows, and thus, bear on the LCP behavior. For a comprehensive study of the Stokes flow in the eccentric cylinder geometry, see Ballal and Rivlin (1976).

Because of the small Reynolds number, the Stokes flow reaches a steady state quickly after start-up; the dimensionless time of the transient is on the order of $10^{-2}$. Figure 3 shows the streamlines and contours of the flow-type parameter in the steady state. There are two groups of closed streamlines, one surrounding the rotating inner cylinder and the other constituting a recirculating eddy in the wide gap. The flow around the inner cylinder is largely shear in nature, whereas the flow in the recirculation zone is rotational. The flow in the area above the inner cylinder, where the two groups of streamlines diverge, is extensional with a negative acceleration along the dividing streamline. In contrast, the

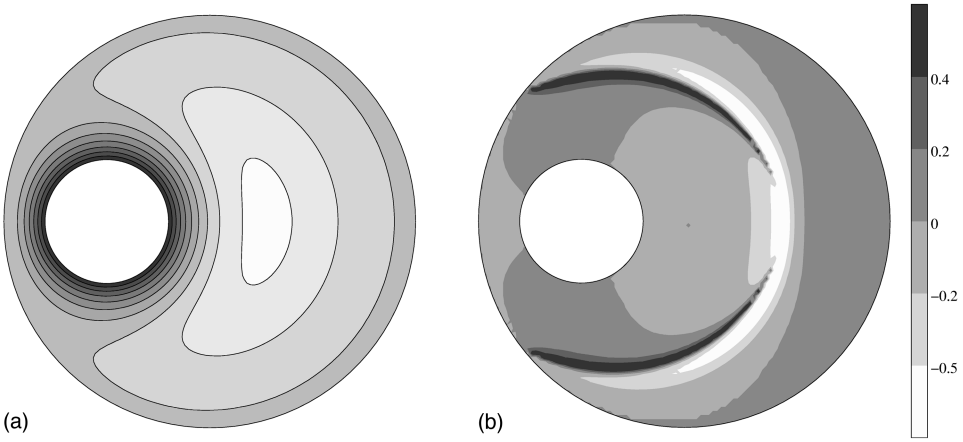


**FIG. 3.** Kinematics of the steady Stokes flow in the eccentric cylinder geometry: (a) streamlines; (b) contours of the flow-type parameter λ. Positive and negative values of λ indicate extensional and rotational flow, respectively. $\lambda = 0$ represents a shear flow. For the definition of λ, see Singh and Leal (1993).

area below the inner cylinder contains a converging flow with positive acceleration along the dividing streamline. Contours of the flow-type parameter consist of three thin strips of nonshear flows surrounded by near-shear flow. The light crescent on the right represents rotational flow associated with the recirculation zone, the minimum of λ occurring on the $x$ axis. The two dark arcs contain extensional flows, with converging and diverging streamlines, respectively.

## IV. STEADY SOLUTIONS OF LCP FLOWS

Previous studies of homogeneous LCP flows [Larson (1990); Chaubal *et al.* (1995)] show that periodic motion of the director (tumbling or wagging) occurs for large values of $U$ and small values of $Pe$, while strong flow and weak nematic strength promote steady alignment with the streamline. These are used as guidelines in the exploration of various LCP regimes in our nonhomogeneous flows. In this section, we present results for $U = 4$ and $Pe = 20$; under these conditions a steady director field is approached in our simulations.

Under flow, the LCP orientation distribution is distorted from the uniaxial shape that it assumes at equilibrium. Then the notion of a director no longer applies. Nevertheless, one can use the principal birefringence axis as an indication of the local orientation [Larson (1990)]. In our paper, the orientation distribution is described approximately by a second-order tensor **A**. Then the eigenvector of **A** corresponding to the largest eigenvalue is a natural choice for representing the preferred orientation of the LCP molecules. We will refer to the unit vector along this eigenvector as the director, with the understanding that the orientation distribution is now biaxially symmetric.

### A. $c = 10$

As mentioned in Sec. II, typical lyotropic LCPs have very large values of $c$. For this preliminary study, we do not strive to simulate a particular LCP system. Instead, the emphasis is on trying to understand the physics of various mechanisms affecting LCP configurations and the fluid flow. Therefore, we have used relatively small values of $c$. To some degree, this avoids the complications of flow modification and simplifies the

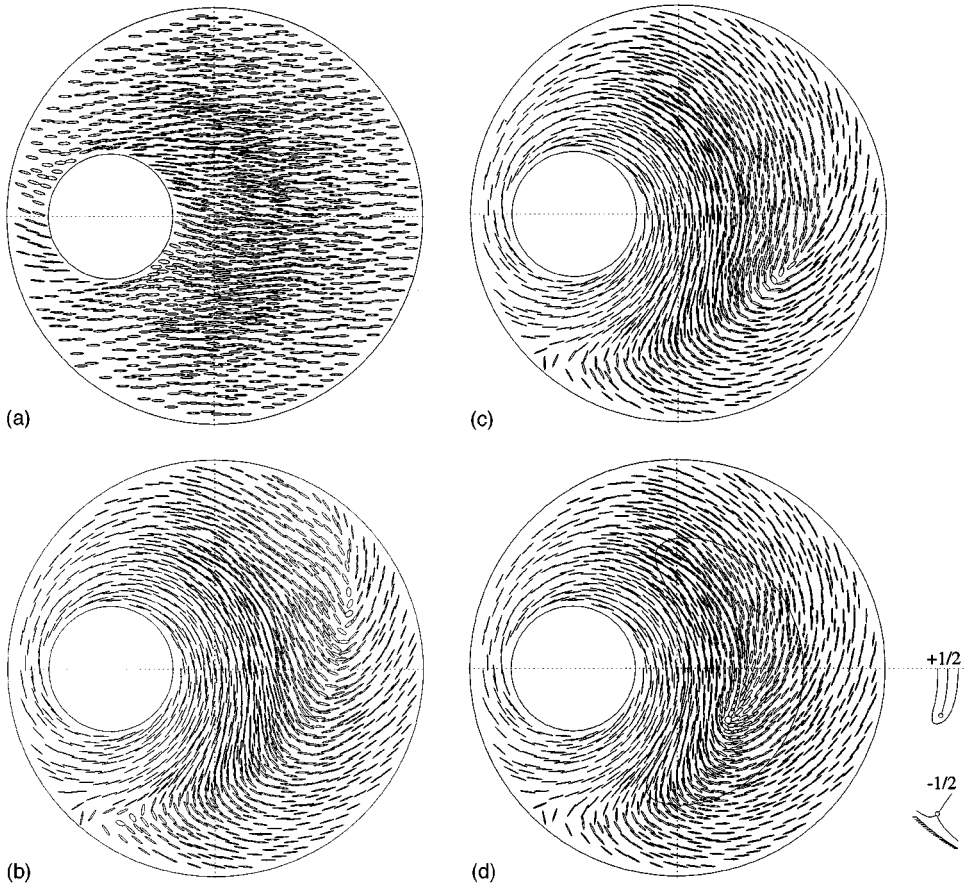


**FIG. 4.** Evolution of the director field for $U = 4$, $Pe = 20$, and $c = 10$. Initially, the director is uniformly aligned with the $x$ axis. (a) Shortly after the start-up at time $t = 0.2$; (b) $t = 24$; (c) $t = 48$; and (d) the steady state at $t = 140$. A streamline is also plotted to illustrate how the director turns with respect to the flow. The sketches show the director lines surrounding the $+1/2$ disclination in the fourth quadrant and the $-1/2$ one in the third quadrant.

task of understanding the behavior of LCPs. The effect of flow modification will be explored within a limited extent in Sec. IV B when we discuss results for $c = 100$.

Initially, the director field is uniformly oriented in either the horizontal or vertical direction. The initial orientation affects the approach to the steady state, but not the steady state itself. With directors initially oriented in the horizontal direction, Fig. 4 shows snapshots of the LCP field during its evolution. Each ellipse represents the configuration tensor at a mesh point; its axes are oriented in the direction of the in-plane eigenvectors, and the length of the semiaxes represents the corresponding eigenvalues. Shortly after start up, the LCP configuration next to the inner cylinder is affected by the flow [Fig. 4(a)]. The director becomes aligned with the circular streamlines, and the beltlike region widens as the effect of the inner cylinder is felt by LCP molecules farther away [Fig. 4(b)]. In the mean time, the recirculation in the wide gap leads to a thin strip resembling a line defect across which the director changes direction rapidly. This is a direct result of the change in sign of the velocity gradient across the strip: the director rotates clockwise to the left of the ''defect'' and counterclockwise to its right. As flow

continues, the strip is healed from the top down [Fig. 4(c)]. Finally, the LCP director field reaches a steady state [Fig. 4(d)].

There are two striking features in the steady-state director field: the asymmetry about the $x$ axis and the disclination-like pattern in the fourth quadrant (see Fig. 1 for the coordinate system). The asymmetry is a manifestation of the alignment behavior of LCPs in converging and diverging extensional flows. Along a recirculating streamline, a polymer molecule encounters a converging flow in the lower-left part of the eddy (see Fig. 3). This aligns the director with the streamline. The flow downstream is roughly shear and the alignment holds. Further downstream, the flow becomes extensional with diverging streamlines in the upper-left part of the eddy. In this region, the director prefers an orientation perpendicular to the streamline, and thus, does not follow the turn of the streamlines. On the right side of the eddy, the flow is again mostly shear and the director is more or less aligned with the streamlines. Therefore, as a result of the varied flow types, the director is aligned with the local streamline everywhere except in the upper-left part of the eddy, where the director is almost perpendicular to the streamlines. In the above discussion, we have referred to streamline and flow-type patterns as depicted in Fig. 3, for the Stokes flow. This is justified because for the relatively small $c$ used here, the flow modification is mild. We will elaborate on flow modifications when discussing results for $c = 100$.

The pattern in the fourth quadrant resembles a disclination of strength $+1/2$. The director orientation changes 180° around the defect core, at which the order parameter is reduced to 0.248; the equilibrium order-parameter $S_{eq} = 0.683$ for $U = 4$. In trying to identify this pattern with a disclination, we realized that a definitive picture of the structure of disclinations in LCPs does not seem to exist. For small-molecule nematics, disclinations have been treated as mathematical singularities with no physical structure [Chandrasekhar (1977); Kléman (1980)]. A model of the defect core was recently proposed by Greco and Marrucci (1992). The ingenuity of this model is that by allowing the order parameter to decrease toward the center of the core, a continuous representation becomes possible. This is especially appropriate for polymeric liquid crystals, whose molecular order is susceptible to external disturbances, e.g., flow or magnetic fields. A ''hedgehog point defect'' was analyzed in this framework and that appears to be the only form of defect whose core structure has been described so far.

The pattern in Fig. 4(d) is considered a disclination because it demonstrates the key features of the Greco–Marrucci model. Toward the center, the ellipsoid representing **A** deforms as described by Greco and Marrucci (1992). The order parameter reaches a minimum at the center of the defect core and the director cannot be defined. Unlike the hedgehog point defect, however, here the orientation distribution need not be isotropic at the center. In fact, it is uniaxial with an oblate shape. To the best of our knowledge, this is the first time that a structured defect core has been identified in a flowing LCP, and it confirms the essence of the Greco–Marrucci model. It is not clear whether such a disclination would appear as a ''thin'' or a ''thick'' thread. Since the orientation distribution varies continuously inside the defect core, the Greco–Marrucci model implies a much blurred distinction between thins and thicks. In particular, it is possible for the orientation distribution to be uniaxially prolate at the center of a half-strength disclination, with the director ''escaping into the third dimension'' [Kléman (1991)]. It would be of interest to test the continuous-core model by microscopic observations of the defect structure in LCP samples.

Outside the defect core, many aspects of the topology of disclinations in small-molecule liquid crystals can be carried over to LCPs. In particular, a conservation theorem holds such that the strength of all disclinations in the domain adds up to a fixed

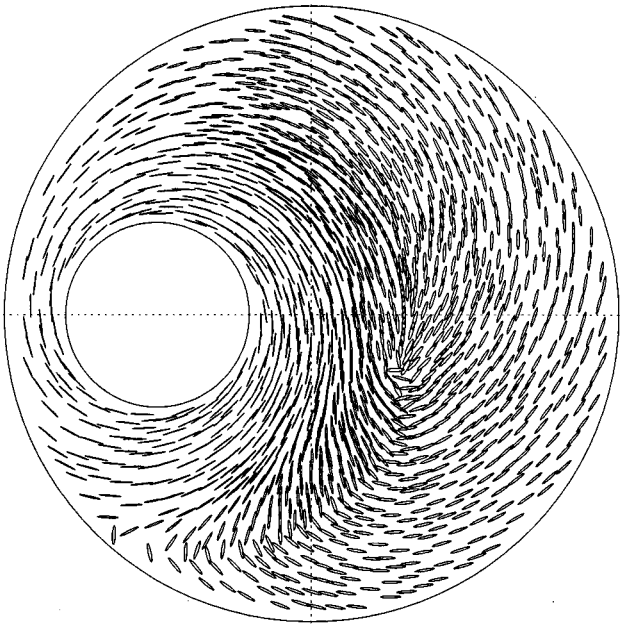

**FIG. 5.** The steady-state director field for $U = 4$, $Pe = 20$, and $c = 100$. Initially, the director is uniformly aligned with the $x$ axis.

number [Kléman (1980)], which is zero in our case. There is a second disclination of strength $-1/2$ in the third quadrant near the outer cylinder. One may also consider the inner cylinder equivalent to a $+1$ disclination and the outer cylinder equivalent to a $-1$ disclination at $\infty$. The zero-sum rule holds regardless of the dynamic behavior of the LCPs, as will be seen in Sec. V.

### B. $c = 100$

In this subsection, we study the effects of larger $c$, especially on the flow field. The steady-state LCP configuration is shown in Fig. 5. It is quite similar to that for $c = 10$, with a pair of $\pm 1/2$ disclinations. But there are some subtle differences, which will be explained by the changes in the flow. Figure 6 compares profiles of the velocity, strain rate, and order parameter along the $x$ axis for $c = 100$, 10, and 0 (Stokes flow). Polymer stress suppresses the fluid flow; the velocity is reduced everywhere in the flow field, most notably in the recirculation zone [Fig. 6(a)]. This effect becomes more severe for larger $c$. Since the velocity is fixed at the surface of the inner cylinder, a larger strain rate arises next to the cylinder [Fig. 6(b)]. This effect is reminiscent of the flow of a dilute polymer solution in a four-roll mill device [Feng and Leal (1997)], in which higher polymer concentration enhances the strength of fluid deformation around the roller but suppresses it farther out. The wriggle at $x \approx 3$ is caused by the relatively large spatial gradient of the polymer configuration in that region (cf. Fig. 5).

The impact of flow modification on the LCP configuration is apparent. For $c = 100$, the order-parameter $S$ is higher than that for $c = 10$, immediately to the right of the inner cylinder [Fig. 6(c)]. Further to the right, however, $S$ drops off more steeply as the flow dies out more rapidly. Interestingly, the difference in $S$ close to the outer cylinder ($5 < x < 10$) is much larger than at the inner cylinder ($x = -2$), though the

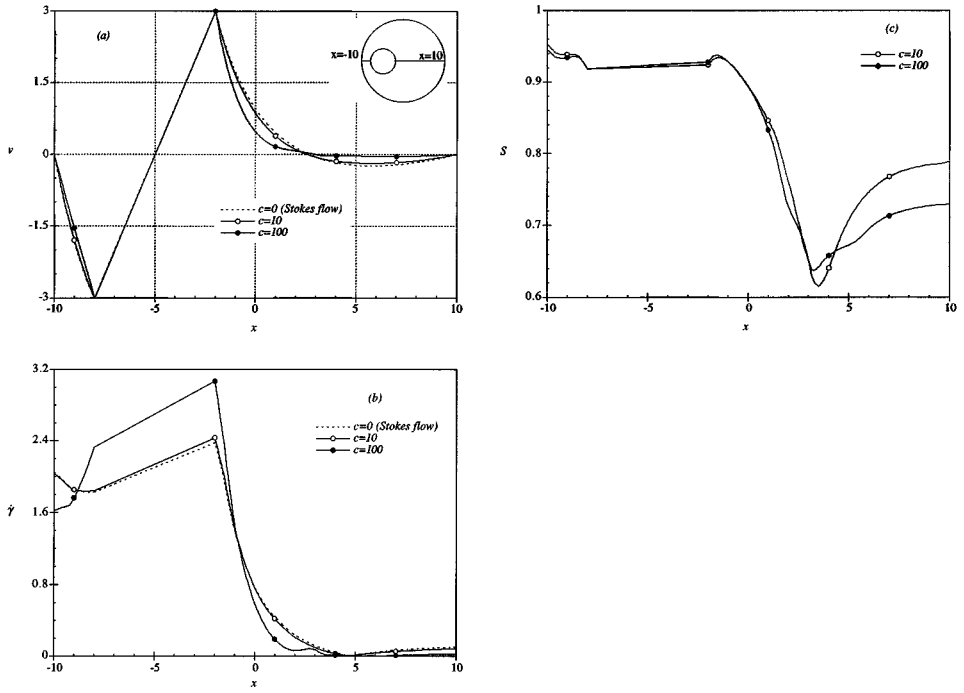


**FIG. 6.** Effects of the concentration parameter $c$ on the steady-state flow and LCP configuration. $U = 4$, and $Pe = 20$. (a) Profiles of the vertical velocity component along the $x$ axis; (b) profiles of the strain rate defined as the magnitude of the strain-rate tensor $\dot{\gamma} = (2\mathbf{D}{:}\mathbf{D})^{1/2}$; and (c) profiles of the order parameter. The straight lines between $x = -8$ and $x = -2$ are within the inner cylinder.

difference in $\dot{\gamma}$ is not as large. This may be an effect of the flow type: the flow is weakly rotational at $x = -2$, but becomes extensional near the outer cylinder (cf. Fig. 3). For both $c = 10$ and $c = 100$, $S$ is above the equilibrium value $S_{\text{eq}} = 0.683$ for all $x$ except a small region at $x \approx 3$. This forms a contrast to simple shear flows, for which $S$ is below $S_{\text{eq}}$ unless $Pe$ is extremely large [Larson (1990)]. Another evidence of the coupling between LCP configuration and flow can be found in the third quadrant below the inner cylinder in Fig. 5. This area consists of two regions in which the director orientation is dictated either by the rotating cylinder (upper left) or by the recirculating eddy (lower right). As compared with Fig. 4(d), the first region expands and pushes the second region to the right. This is evidently a result of the reduced strength of the eddy depicted in Fig. 6(b).

### C. Log rolling

If initially the director field is uniformly oriented in the $z$ direction (perpendicular to the flow plane), a different steady-state configuration is reached (Fig. 7). The director is flow aligned in the region surrounding the inner cylinder and a log-rolling state prevails in the wide gap. A similar solution was obtained by Wang (1996) for a Couette flow. There is a sharp transition between the log-rolling and flow-aligning regions; the eigenvalue of $\mathbf{A}$ corresponding to the out-of-plane eigenvector shrinks as one moves from the log-rolling region toward the inner cylinder. The larger in-plane eigenvalue grows and becomes the largest of the three inside the flow-aligning region. This picture is consistent with the calculations of Larson and Öttinger (1991) in simple shear flows, which predict

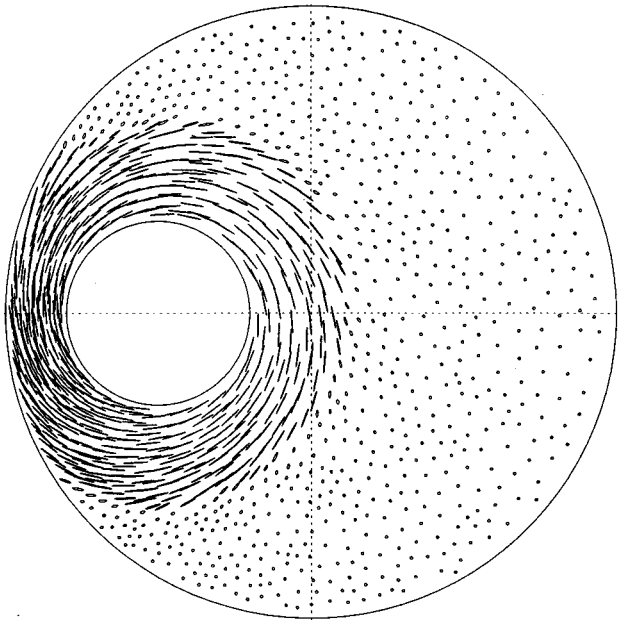

**FIG. 7.** The steady-state director field for $U = 4$, $Pe = 20$, and $c = 100$. Initially, the director is uniformly aligned with the $z$ axis (perpendicular to the flow plane).

log rolling as a stable solution at low shear rate, but flow aligning to be the sole attractor at large shear rate. Quantitative comparison is hampered by the nonshear flow types in our problem.

The boundary between the flow-aligning and log-rolling domains can be considered a surface of twist disclinations, or a ''wall'' [Donald and Windle (1992)]. The orientation distribution becomes uniaxially oblate (disklike), where the eigenvalue associated with the out-of-plane eigenvector equals the larger of the in-plane eigenvalues; the director degenerates. This is also where the order parameter drops to a minimum (Fig. 8). In reality, such disclination surfaces appear most often during a transformation from a homeotropic to a planar configuration between solid walls.

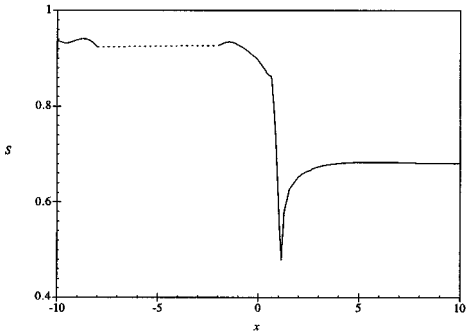


**FIG. 8.** The profile of the order-parameter $S$ along the $x$ axis in the steady state shown in Fig. 7. The minimum of $S$ at $x = 1.16$ indicates the ''wall'' separating the flow-aligning and log-rolling regimes. The dash line between $x = -8$ and $x = -2$ is inside the inner cylinder.

## V. A POLYDOMAIN SOLUTION WITH DIRECTOR TUMBLING

In this section, we consider the start-up flow of a lyotropic LCP for $U = 20$, $Pe = 100$, and $c = 10$. As mentioned before, the relatively small $c$ value is used to avoid the complication of severe flow modification. Figure 9 shows the evolution of the LCP configuration after start-up. (We have made a video from these numerical results, which gives a better representation of the evolving LCP configuration and disclination formation. The video is available from the authors upon request.)

Initially, the development of the director field is similar to that shown in Fig. 4, although the order parameter is higher owing to the larger $U$. As in Fig. 4(b), an arc-shaped defect forms as a result of the recirculating eddy [Fig. 9(b)]. This arc seems to contain multiple defect cores; the sketch shows two pairs of $\pm 1/2$ disclinations on top of a $+1/2$ disclination. We should note that the accuracy of such a sketch is limited by the resolution of the numerical results. If a defect core does not fall on a grid point, its existence is inferred from the director orientation in the neighborhood. Besides, additional pairs of $\pm 1/2$ disclinations may exist which are too close together to be detected. The strength of all disclinations in the arc adds up to $+1/2$, and the total strength of all disclinations in the plane equals zero.

As the flow progresses, the pairs of $\pm 1/2$ disclinations in the arc cancel, leaving only the $+1/2$ disclination at the bottom, which travels to the lower left [Fig. 9(c)]. Meanwhile, the director starts to tumble in the upper part of the eddy. This gives birth to a pair of $\pm 1/2$ disclinations as shown in the sketch. As the tumbling zone grows and assumes a kidney shape [Fig. 9(d)], the $-1/2$ disclination travels downward along the left boundary of the tumbling zone and the $+1/2$ disclinations along its right boundary. In the upper part of the tumbling zone, the boundary starts to heal; the director inside has tumbled through 180° and its orientation is again in accord with its neighbors outside. When the $-1/2$ disclination eventually arrives at the bottom of the tumbling zone [Fig. 9(e)], it meets the $+1/2$ disclination that is the remnant of the arc in Fig. 9(b). These two disclinations annihilate each other, leaving the $+1/2$ disclination traveling down the right boundary of the tumbling zone [Fig. 9(f)]. Finally, the tumbling approaches the end of the cycle in Fig. 9(g) and a new cycle is about to start as depicted in Fig. 9(c). Note that at any moment, the total strength of all disclinations is conserved.

Figure 10 shows the periodic change of the order-parameter $S$ and the orientation angle $\theta$ at $(x,y) = (3,0)$ inside the tumbling zone. The $S$ value oscillates as the principal axis of $\mathbf{A}$ is alternately compressed and stretched by the flow, much like in a simple shear flow [Larson (1990)]. The period is about $T = 53$, and does not vary much throughout the tumbling zone. Immediately outside the tumbling zone is a belt-shaped region in which the director wags. Further out, the director field is steady and resembles that in Fig. 4(d). The tumbling and wagging behavior is mainly caused by the rotational flow type in the recirculation region, consistent with the effect that Chaubal *et al.* (1995) observed in homogeneous flows.

The most remarkable feature of Fig. 9 is the polydomain structure caused by director tumbling. The exact meaning of a ''domain'' was the subject of a debate at a Faraday Discussion more than a decade ago. In an analogy to ferromagnetism, Windle (1985) defined a domain ''as a region within which an orientation parameter varies no more than slowly with position, compared with its rapid variation at the delineating boundaries.'' Later observations of thin LCP films corroborated the fact that the orientation is roughly uniform within a domain [Wood and Thomas (1986)]. The tumbling zone in Fig. 9 fits this definition of a domain. Furthermore, Wood and Thomas (1986) discovered that the boundary of a domain consists of an even number of discrete disclination lines, normal to

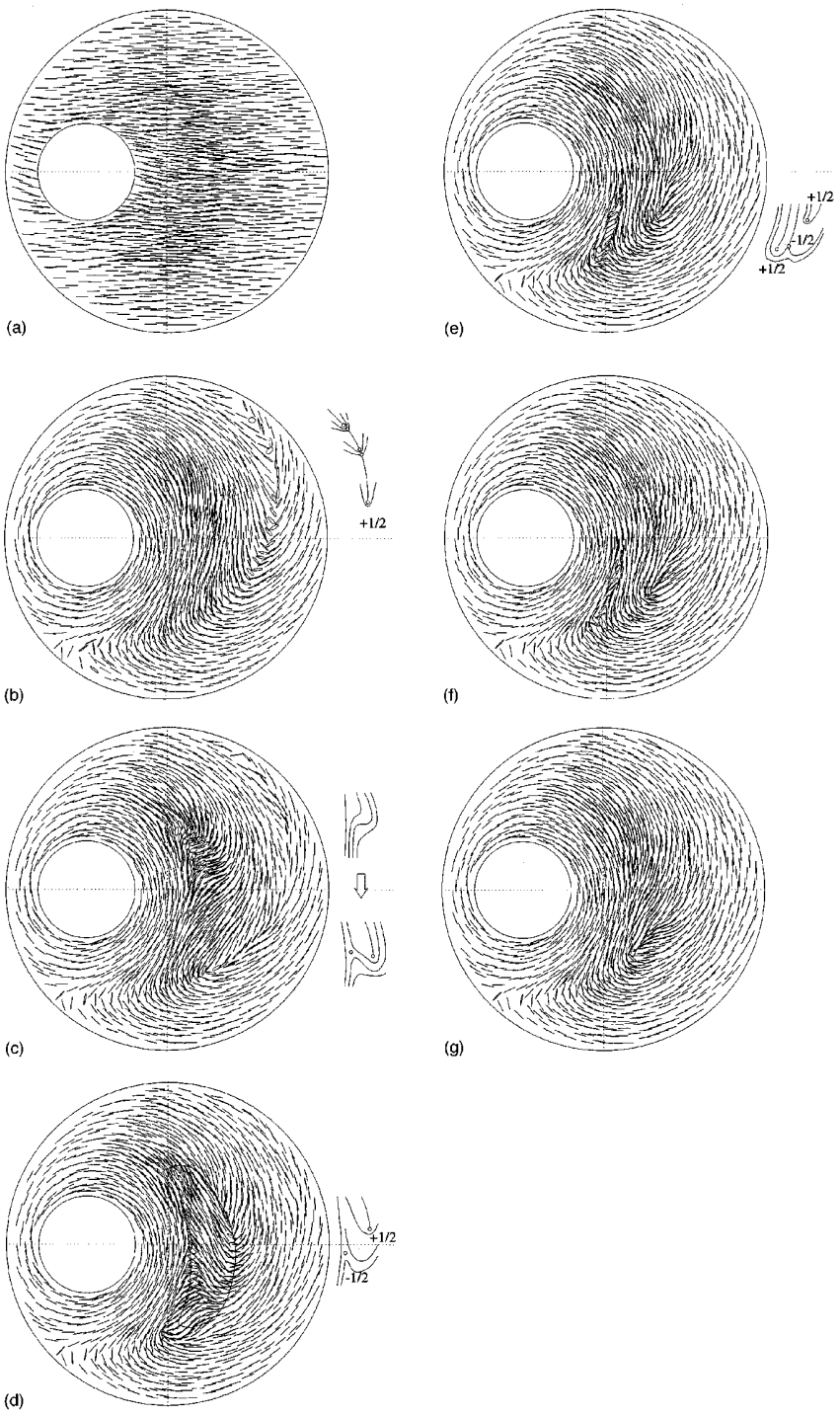


**FIG. 9.** Evolution of the director field for $U = 20$, $Pe = 100$, and $c = 10$. Initially, the director is uniformly aligned with the $x$ axis. The sketches to the right of some plots show the director lines around disclinations. (a) Shortly after the start-up at time $t = 0.2$, (b) $t = 33$, and (c) $t = 49$; the upper sketch shows director lines at this time and the lower one illustrates the two disclinations to emerge shortly afterwards. (d) $t = 65$; the maximum extent of the tumbling domain is indicated. (e) $t = 81$, (f) $t = 85$, and (g) $t = 93$.

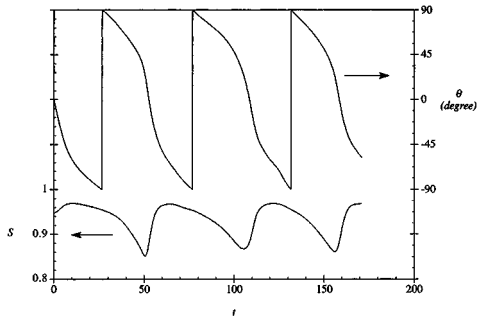


**FIG. 10.** The periodic change of the order-parameter $S$ and the orientation angle $\theta$ at $(x,y) = (3,0)$ inside the tumbling zone. $U = 20$, $Pe = 100$, and $c = 10$. The equilibrium order-parameter $S_{\text{eq}} = 0.948$.

the LCP film, with alternating $+1/2$ and $-1/2$ strength; across the boundary the director undergoes rapid but continuous rotation except in the vicinity of the disclination cores. This description of the domain boundary agrees perfectly with that depicted in Fig. 9(d). Though the photographs of Wood and Thomas (1986) show the boundary as straight line segments connecting neighboring disclinations, this configuration is not unique. In fact, Fig. 9(d) shows curved boundaries containing only one pair of $\pm 1/2$ disclinations. Our tumbling domain is topologically equivalent to the domain sketched in Fig. 11.

Another feature of the tumbling domain is that the order-parameter $S$ drops on the domain boundary, where the director orientation changes rapidly. This is expected in the vicinity of the defect cores, but appears to be true even away from the disclinations. It is not clear whether there is an intrinsic connection between the large gradient of the director orientation and reduced molecular order. There seems to be no experimental data on the variation of $S$ across a domain boundary.

## VI. DISCUSSION AND CONCLUSION

The two main results of this paper are the generation of disclinations by flow and the formation of a polydomain structure bounded by disclinations. The key element in these events is the nonhomogeneity of the flow field. In particular, director tumbling in the rotational eddy is responsible for forming the domain. In experiments, however, disclinations have been observed to emerge and multiply in simple shear flows [Larson and Mead (1992); Mather (1994)]. It appears that in these experiments, disclinations are

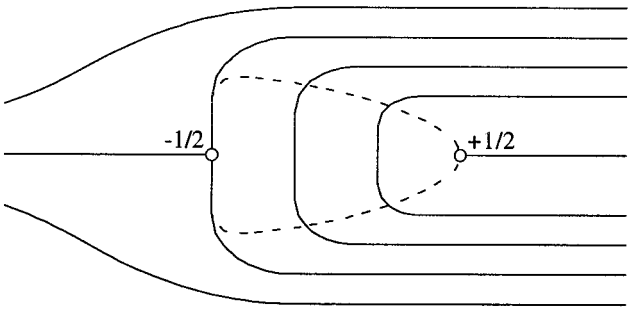


**FIG. 11.** A sketch illustrating a domain whose boundary (the dash loop) contains a pair of $\pm 1/2$ disclinations. The director orientation is roughly uniform inside the domain and differs from the prevalent orientation outside.

caused by initial nonhomogeneity of the polymer configuration. Gradient elasticity, which reduces to the Frank elasticity in the limit of small distortions [Marrucci and Greco (1991, 1993)], makes possible director anchoring at solid surfaces or at residual defect cores in apparently relaxed samples. When a shear flow is applied, the nonhomogeneity of the LCP configuration prohibits uniform tumbling of the director field and eventually leads to disclinations.

Hence, the nonhomogeneity in the fluid flow and that in the polymer configuration are two independent agents that may cause disclinations. Note that gradient elasticity is not included in our simulations. A consequence of this omission is the periodic healing of the boundary of the tumbling domain. No elastic energy builds up as the director field gets splayed and bent at the boundary. Therefore, part of the boundary disappears periodically when the difference in orientation angle across the boundary reaches a multiple of 180°. In reality, more disclinations must arise at the boundary to release the mounting elastic energy: if the director degenerates or escapes into the third dimension, the continuous rotation of the director on one side of the boundary will not cause unlimited winding. This mechanism may explain the phenomenon that continued shear leads to proliferation of disclinations and reduction of the domain size [Alderman and Mackley (1985); Larson and Mead (1992)]. The absence of the elastic stress in our simulations may be the principal reason that our tumbling domain retains a large size as compared to the domains found in experiments.

Obviously, the next task is to incorporate the gradient elasticity into the Doi theory, and the nonlocal nematic potential of Marrucci and Greco (1991, 1993) may serve this purpose. With the introduction of a $\nabla^2\mathbf{A}$ term in the nematic potential, the LCP configuration is correlated between neighboring streamlines, and its evolution now follows an elliptic equation [cf. Eq. (6)]. In complex flows, one will be able to include wall anchoring as a boundary condition. Flow-induced disclinations may arise from the flow kinematics or the gradient elasticity, and the two mechanisms may interact.

Finally, the findings of this study can be summarized as follows:

(1) The LCP director exhibits steady or periodic behavior depending on the nematic strength parameter $U$, the Peclet number $Pe$, the local flow-type parameter $\lambda$, and the deformation history. The effects of $U$, $Pe$ and $\lambda$ are consistent with previous studies of homogeneous flows. The deformation history is determined by the kinematics of the flow.
(2) The nonhomogeneity of the flow gives rise to disclinations of $\pm 1/2$ strength. The structure of the defect core corroborates the main features of the continuous-core model of Greco and Marrucci (1992).
(3) Director tumbling in the rotational flow region produces a polydomain structure. The boundary of the tumbling domain consists of a pair of $\pm 1/2$ disclinations in agreement with the observations of Wood and Thomas (1986).

The last two conclusions are subject to the caveat that the elastic stress due to spatial gradients in the director field has not been taken into account.

## ACKNOWLEDGMENTS

The authors thank the referees for their insightful suggestions, one of which, in particular, led to a clearer presentation of the disclinations. This research was supported by grants from the Fluid Dynamics program at the National Science Foundation and by the Materials Research Laboratory at UCSB. The computation was done at the NSF Supercomputer Centers in San Diego and Pittsburgh. The authors thank their colleagues Charu Chaubal and Johan Remmelgas for their help with the project and many discussions.

## References


Alderman, N. J. and M. R. Mackley, ''Optical textures observed during the shearing of thermotropic liquid-crystal polymers,'' Faraday Discuss. Chem. Soc. **79**, 149–160 (1985).

Armstrong, R. C., S. Ramalingam, and D. E. Bornside, ''A finite-element model to predict structure development in spinneret flow of liquid-crystalline polymers,'' SPE ANTEC Proc. 2590–2594 (1995).

Baek, S.-G., J. J. Magda, and S. Cementwala, ''Normal stress differences in liquid crystalline hydroxypropylcellulose solutions,'' J. Rheol. **37**, 935–945 (1993a).

Baek, S.-G., J. J. Magda, and R. G. Larson, ''Rheological differences among liquid-crystalline polymers. I. The first and second normal stress differences of PBG solutions,'' J. Rheol. **37**, 1201–1224 (1993b).

Baleo J.-N. and P. Navard, ''Rheo-optics of liquid crystalline polymers in complex geometries,'' J. Rheol. **38**, 1641–1656 (1994).

Ballal, B. Y. and R. S. Rivlin, ''Flow of a Newtonian fluid between eccentric rotating cylinders: Inertial effects,'' Arch. Ration. Mech. Anal. **62**, 237–294 (1976).

Bedford, B. D. and W. R. Burghardt, ''Molecular orientation and instability in plane Poiseuille flow of a liquid crystalline polymer,'' J. Rheol. **38**, 1657–1679 (1994).

Bedford, B. D. and W. R. Burghardt, ''Molecular orientation of a liquid-crystalline polymer solution in mixed shear-extensional flow,'' J. Rheol. **40**, 235–257 (1996).

Bhave, A. V., R. C. Armstrong, and R. A. Brown, ''Kinetic theory and rheology of dilute, nonhomogeneous polymer solutions,'' J. Chem. Phys. **95**, 2988–3000 (1991).

Chandrasekhar, S., *Liquid Crystals* (Cambridge University Press, Cambridge, UK, 1977).

Chaubal, C. V., L. G. Leal, and G. H. Fredrickson, ''A comparison of closure approximations for the Doi theory of LCPs,'' J. Rheol. **39**, 73–103 (1995).

Doi, M., ''Molecular dynamics and rheological properties of concentrated solutions of rodlike polymers in isotropic and liquid crystalline phases,'' J. Polym. Sci. Polym. Phys. Ed. **19**, 229–243 (1981).

Doi, M. and S. F. Edwards, *The Theory of Polymer Dynamics* (Oxford, London, 1986).

Donald, A. M. and A. H. Windle, *Liquid Crystalline Polymers* (Cambridge University Press, Cambridge, UK, 1992).

Doraiswamy, D. and A. B. Metzner, ''The rheology of polymeric liquid crystals,'' Rheol. Acta **25**, 580–587 (1986).

Feng, J. and L. G. Leal, ''Numerical simulations of the flow of dilute polymer solutions in a four-roll mill,'' J. Non-Newtonian Fluid Mech. **72**, 187–218 (1997).

Greco, F. and G. Marrucci, ''Molecular structure of the hedgehog point defect in nematics,'' Mol. Cryst. Liq. Cryst. Sci. Technol., Sect. A **210**, 129–141 (1992).

Grizzuti, N., S. Guido, V. Nastri, and G. Marrucci, ''Velocity profiles in rectangular channel flow of liquid crystalline polymer solutions,'' Rheol. Acta **30**, 71–76 (1991).

Kléman, M., ''The general theory of disclinations,'' in *Dislocations in Solids*, edited by F. R. N. Nabarro (North-Holland, Amsterdam, 1980), Chap. 22, pp. 243–297.

Kléman, M., ''Defects and textures in liquid crystalline polymers,'' in *Liquid Crystallinity in Polymers*, edited by A. Ciferri (VCH, New York, 1991), Chap. 10, pp. 365–394.

Larson, R. G., ''Arrested tumbling in shear flows of liquid crystalline polymers,'' Macromolecules **23**, 3983–3992 (1990).

Larson, R. G., ''Roll-cell instabilities in shearing flows of nematic polymers,'' J. Rheol. **37**, 175–197 (1993).

Larson, R. G. and M. Doi, ''Mesoscopic domain theory for textured liquid crystalline polymers,'' J. Rheol. **35**, 539–563 (1991).

Larson, R. G. and D. W. Mead, ''Development of orientation and texture during shearing of liquid-crystalline polymer,'' Liq. Cryst. **12**, 751–768 (1992).

Larson, R. G. and D. W. Mead, ''The Ericksen number and Deborah number cascades in sheared polymeric nematics,'' Liq. Cryst. **15**, 151–169 (1993).

Larson, R. G. and H. C. Öttinger, ''Effect of molecular elasticity on out-of-plane orientation in shearing flows of liquid crystalline polymers,'' Macromolecules **24**, 6270–6282 (1991).

Leslie, F. M., ''Theory of flow phenomena in liquid crystals,'' Adv. Liq. Cryst. **4**, 1–81 (1979).

Magda, J. J., S.-G. Baek, K. L. DeVries, and R. G. Larson, ''Shear flows of liquid crystal polymers: Measurements of the second normal stress difference and the Doi molecular theory,'' Macromolecules **24**, 4460–4468 (1991).

Marrucci, G., ''Rheology of rodlike polymers in the nematic phase with tumbling or shear orientation,'' Rheol. Acta **29**, 523–528 (1990).

Marrucci, G. and F. Greco, ''The elastic constants of Maier–Saupe rodlike molecule nematics,'' Mol. Cryst. Liq. Cryst. **206**, 17–30 (1991).

Marrucci, G. and F. Greco, ''A molecular approach to the polydomain structure of LCPs in weak shear flows,'' J. Non-Newtonian Fluid Mech. **44**, 1–13 (1992).

Marrucci, G. and F. Greco, ''Flow behavior of liquid crystalline polymers,'' Adv. Chem. Phys. **86**, 331–404 (1993).

Marrucci, G. and P. L. Maffettone, ''Nematic phase of rodlike polymers. II. Polydomain predictions in the tumbling regime,'' J. Rheol. **34**, 1231–1244 (1990).

Mather, P. T., ''Shear Flow Behavior of Tumbling and Flow-Aligning Nematic Liquid Crystals,'' Ph.D. thesis, University of California, Santa Barbara (1994).

Mori, N., Y. Tsuji, K. Nakamura, and C. Yoshikawa, ''Numerical simulations of the flow of liquid crystalline polymers between parallel plates containing a cylinder,'' J. Non-Newtonian Fluid Mech. **56**, 85–97 (1995).

Onogi, S. and T. Asada, ''Rheology, and rheo-optics of polymer liquid crystals,'' in *Rheology*, edited by G. Astarita, G. Marrucci, and L. Nicholais, Proc. 8th Int'l Congr. Rheol., Naples (Plenum, New York, 1980), Vol. I, pp. 127–147.

Ophir, Z. and Y. Ide, ''Injection molding of thermotropic liquid crystal polymers,'' Polym. Eng. Sci. **23**, 792–796 (1983).

Pieranski, P., E. Guyon, and S. A. Pikin, ''Nouvelles instabilités de cisaillement dans les nématic,'' J. Phys. (Paris) Colloq. **37**, 3–6 (1976).

See, H., M. Doi and R. G. Larson, ''The effect of steady flow fields on the isotropic–nematic phase transition of rigid rod-like polymers,'' J. Chem. Phys. **92**, 792–800 (1990).

Singh, P, and L. G. Leal, ''Finite-element simulation of the start-up problem for a viscoelastic fluid in an eccentric rotating cylinder geometry using a third-order upwind scheme,'' Theor. Comput. Fluid Dyn. **5**, 107–137 (1993).

Ugaz, V. M., D. K. Cinader, and W. R. Burghardt, ''X-ray scattering investigation of the origin of region I shear thinning in concentrated solutions of poly(benzyl glutamate),'' Soc. Rheol. 68th Ann. Meeting. Galveston, Texas. Feb. 16–20, 1997.

Walker, L. and N. Wagner, ''Rheology of region I flow in a lyotropic liquid-crystal polymer: The effects of defect texture,'' J. Rheol. **38**, 1525–1547 (1994).

Wang, Q., ''Couette flows of liquid crystal polymers,'' in *Rheology and Fluid Mechanics of Nonlinear Materials*, edited by D. A. Siginer and S. G. Advani (ASME, New York, 1996), AMD-Vol. 217, pp. 109–115.

Windle, A. H., Faraday Discuss. Chem. Soc. **79**, 186 (1985).

Wood, B. A. and E. L. Thomas, ''Are domains in liquid crystalline polymers arrays of disclinations?,'' Nature (London) **324**, 655–657 (1986).